4ICEGE Thessaloniki-GREECE 2007

4th International Conference on
Earthquake Geotechnical Engineering
June 25-28, 2007
Paper No. ++++

DYNAMIC AND STATIC LIQUEFACTION POTENTIAL OF A SILTY SAND FROM BOSTANJ, SLOVENIA

Stanislav LENART[1], Gregor VILHAR[2]

ABSTRACT

The construction of the accumulation reservoir caused the submergence of the railway line embankment. Therefore, field and laboratory tests of the embankment material were carried out to examine the stability conditions. The embankment consists of a loose silty sand layer with fines content of 30%, whose possible liquefaction triggering raised questions. Consequently, the laboratory tests consisted of undrained static triaxial compression tests, direct shear box tests, bender element tests, cyclic triaxial tests and cyclic simple shear tests, and were focused on liquefaction behaviour of the loose silty sand material under static and dynamic loading conditions. Some field test measurements were also performed. The test results showed that in-situ state of the examined material is close to the critical state line in void ratio-effective stress plane, hence during shearing both contractive and dilative responses are possible. Moreover, the most unfavourable in-situ stress state in *p*'-*q* plane lies very close to the peak/instability line. Therefore, the flow liquefaction of the material can not be excluded. A simple relation connecting the peak deviator stress and peak mean effective stress with mean effective stress after consolidation and state parameter was derived from the results of undrained triaxial tests. It might be used for modelling of instability points. Cyclic triaxial and simple shear tests were used to define the material susceptibility to liquefaction and cyclic mobility. The measured amplitudes of the acceleration caused by train passings are supposed not to be able to cause the cyclic mobility in the layer of a silty sand.

Keywords: flow liquefaction, cyclic mobility, steady state line, instability line, silty sand

INTRODUCTION

The railway connection between the capitals of Slovenia and Croatia runs along the alluvial areas of the Sava river. Near the town of Bostanj in Slovenia, the accumulation reservoir of the new hydro power plant was under construction. The raise of the river water level was expected to cause also the raise of the ground water level in the railway embankment. Therefore, the stability analyses considering new ground water level were required by the owner of the railway (Lenart and Petkovsek, 2006; Lenart et al., 2005). Field and laboratory tests were carried out before the upheaval of the water in order to get the input parameters for the analyses. Sample borings showed that the geological structure of the embankment under the railway track is heterogeneous. Above the bedrock, it comprises mostly of clayey and silty gravel, clay and silt of low plasticity and silty sand, which is in a loose state. While according to literature (e.g. Castro (1975); Castro and Poulos (1977); Ishihara (1993), collection of papers edited by Lade and Yamamuro (1999)), the saturated loose sands, silty sands and silts are known to be susceptible to liquefaction failures, the most attention was paid to the behaviour of the material from the silty sand layer in the perspective of the static liquefaction (flow failure) and cyclic mobility.

[1] Slovenian National Building and Civil Engineering Institute (ZAG), Ljubljana, Slovenia, Email: stanislav.lenart@zag.si
[2] Slovenian National Building and Civil Engineering Institute (ZAG), Ljubljana, Slovenia

The term static liquefaction (flow failure) refers to a quick increment of pore water pressure followed by a sudden loss of strength after the peak value of deviator stress is reached, until a residual/steady state strength is reached. Beyond the peak, the material strength is decreasing and the instability occurs when the external load exceeds the decreasing strength. The existence of the descending part of the material response is associated with the tendency for loosely packed granular materials to contract (densify), which is prevented by the constant-volume constraint in undrained loading. This results in a pore-water pressure build up. In medium dense granular materials, the descending part of the deviatoric stress is usually followed by a rising part until the final, steady state is reached. The corresponding response is called "limited liquefaction".

Cyclic mobility occurs when the vibratory disturbance acting upon a granular mass causes the momentary drops of effective stress to zero. It can develop under conditions where the static shear stress is smaller than the steady-state shear strength. The vibrations induce a decrease in volume irrespective of the density or the degree of saturation of the material. This results in a progressive pore pressure build up in the case of the saturated granular material under undrained conditions, which moves the effective stress path in the triaxial *p'-q* plane relatively quickly to the left, eventually oscillating along the compression and extension portions of the drained failure envelope. During cycling a point is reached, termed as "initial liquefaction" (Seed and Lee, 1966), after which the value of pore pressure, at zero deviator stress, is momentarily equal to the confining stress. After this point, the strains during each subsequent cycle become progressively larger, while during each cycle the pore pressure becomes equal to the confining pressure. Even though the initial liquefaction is the state of zero effective stress, it should not be taken to imply that the soil has no shear strength, while in each cycle the strength is rebuilding. Significant permanent damaging deformations, which are limited, may accumulate during cyclic mobility, but flow failure can not occur, unless there are static shear stresses that are larger than steady state strength. On the other hand, flow failures are characterized by a sudden loss of strength and a rapid development of large deformation.

SITE EXPLORATION AND FIELD CONDITIONS

At the time of the beginning of a site exploration the river level had not been raised yet. Several boreholes of depths 6-10 m were drilled in the embankment near the railway tracks. Figure 1 shows the cross section of the embankment at the position km 490+070. The raise of a water river level for about 7 m can be seen. The final river level is just 1.3 m below the railway tracks. The silty sand and silt layer (SM/ML) which is taken into consideration in this paper lies at the depths of 1.8 to 6.0 m, with varying thicknesses of 1.0 to 2.5 m along the railway line.

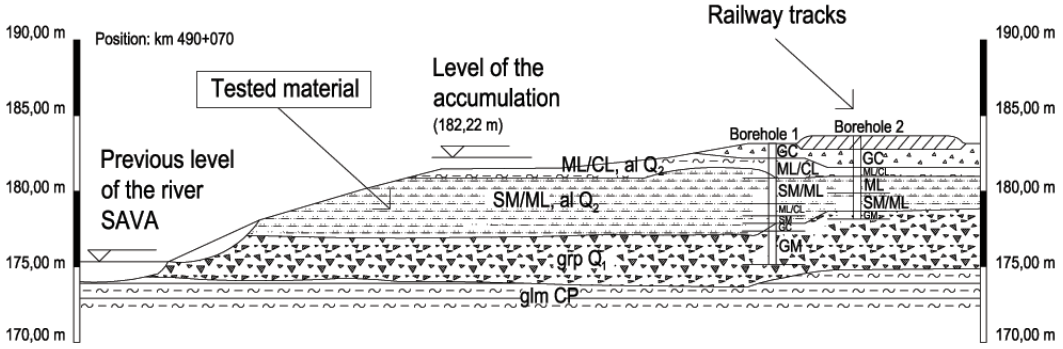

Figure 1. One cross section of the embankment

Retrieved silty sand specimens from the borehole cores were subjected to a full suite of laboratory index tests including sieve, hydrometer, density, particle specific gravity, liquid and plastic limits, water content and coefficient of permeability. In addition, direct shear box and monotonic undrained

triaxial tests were performed to get the strength parameters, along with the oedometer tests to get oedometer moduli. Summary of the results is given in Table 1. An evaluation of Atterberg limits indicated the non-plastic character of the fines. The grain size distribution of the silty sand material is shown on Figure 2.

Table 1. Physical properties of the undisturbed silty sand.

Characteristic	Sign and unit	Value
Dry unit weight	γ_d (kN/m^3)	15.7 – 16.5
Water content	w (%)	17.8 – 23.8
Particle specific gravity	G_s (-)	2.69 – 2.75
Void ratio	e (-)	0.63 – 0.72
Degree of saturation	S_r (-)	0.75 – 0.90
Coefficient of permeability	k (cm/s)	9×10^{-8}
Angle of internal friction	φ (^{o})	30 – 35
Cohesion	c (kPa)	0 – 10
Fines content (<0.063mm)	*FC (%)*	26 – 32

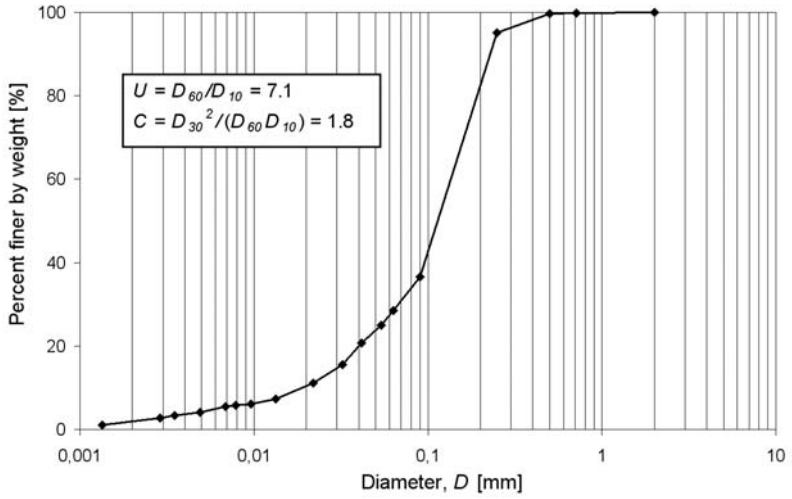

Figure 2. Grain size distribution of silty sand tested

In 6 boreholes SPT measurements were carried out. Longitudinal and shear wave velocities (v_p and v_s) were measured using shallow refraction and analysis of the Rayleigh waves (measurement of the seismic noise). The results of field tests are presented in Table 2. According to the field conditions and expected changes in the ground water level, the danger of liquefaction or cyclic mobility occurrence in the silty sand layer in the embankment was detected. Therefore some further laboratory tests were performed to determine liquefaction susceptibility.

Table 2. Summary of the results of SPT and geophysical tests in the field.

SPT corrected blow count (material was not submerged)	$(N_1)_{60}$	5.8 – 6.3
Velocity of longitudinal waves	v_p (m/s)	250 – 420
Velocity of shear waves	v_s (m/s)	190 – 290

Cyclic mobility was evaluated based on the acceleration measurements at the surface and in the silty sand layer due to the train passings and it seems unlikely to occur. Accelerations were measured during and after the accumulation reservoir filling using three dimensional accelerometers. Figure 3 shows a part of the results of these measurements in one of the boreholes. It can be seen that the vertical acceleration is larger than horizontal, but the difference is reduced in depth. Moreover, all accelerations are substantially reduced in the silty sand layer comparing to the surface accelerations. Maximum measured vertical acceleration in the silty sand layer is 0.095g and at the surface 0.72g.

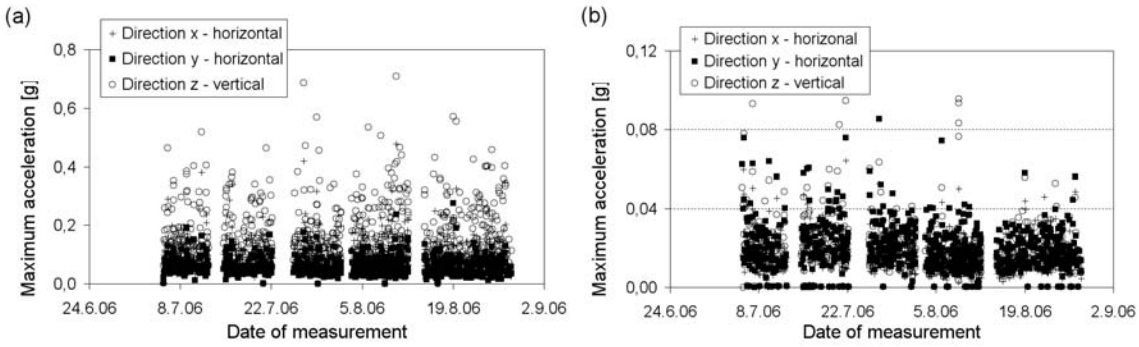

Figure 3. Borehole acceleration measurements at the surface (a) and at the depth (b) of the silty sand

Another source of more crucial acceleration are the earthquakes. Slovenia is seismically medium active area. The design ground acceleration a_g around Bostanj area on the ground type A (Eurocode 8) is 0.15g (Lapajne et al., 2001). The ground below the railway tracks can be classified as type E ground, with the corresponding soil factor S equal to 1.7 (Eurocode 8). Therefore, the danger of seismically induced liquefaction in the silty sand layer is treated in continuation.

FURTHER LABORATORY TESTS

The silty sand was more carefully examined by a series of monotonic and cyclic laboratory tests. The aim of the tests was to determine liquefaction susceptibility of the material, its static and dynamic properties. All the specimens were reconstituted from the silty sand material of the embankment base.

Monotonic tests

The monotonic tests consisted of direct shear box tests, undrained triaxial compression tests and piezoelectric bender element tests.

Direct shear box tests

The sample dimensions were 60 mm x 60 mm at the cross section and 20 mm in height. The water content of the material was 20%. The density of the material was varied so that the desired range of specimen void ratios after the consolidation was accomplished. The aim of the tests was to determine the connection between void ratio with almost no volume change during shearing and effective vertical stress, σ_v'. These void ratios (usually called the critical void ratios, e_{crit}) characterize the transition between the contractive and dilative behaviour during shearing. The locus of points connecting the e_{crit} and corresponding σ_v' defines the critical state line (Schofield and Wroth, 1968) in e - σ_v' plane. If the material state is on the left ('dry') side of the critical state line, the dilative behaviour during shearing is anticipated. On the other hand, if the material state is on the right ('wet') side, contracitve behaviour ensues. In the field, under stress-controlled shearing, the contractive behaviour may result in the sudden loss of strength, which can lead to liquefaction.

According to the results of direct shear box tests of reconstituted specimens, the critical state line in e - $\log\sigma_v$' plane is drawn (Figure 4) along with two one-dimensional compression lines from oedometer tests on undisturbed samples. The reason for the difference in slopes of lines seems to be because an insufficiently high stress in one-dimensional compression to reach the normal compression line. The similar difference in slopes of critical state line and isotropic compression line in *e-p'* plane is presented in the following section.

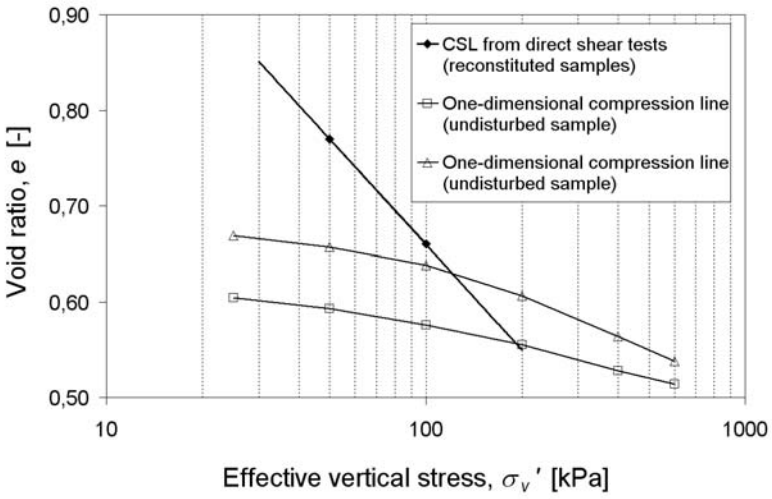

Figure 4. The critical state line (CSL) in *e* - logσ_v' plane deduced from the direct shear box tests (reconstituted samples) and two one-dimensional compression lines from oedometer tests (undisturbed samples)

Monotonic triaxial tests

Undrained triaxial compression tests under monotonic loading conditions were conducted on the reconstituted saturated silty sand specimens. The objective of the tests was to observe the behaviour of the material under different effective confining pressures and void ratios. The specimens were 35 mm in diameter and 70 mm in height. They were prepared using moist placement method. According to the required initial void ratio, the wet silty sand was divided into five portions of equal weight and placed into the mould in five layers. The water content of the material was chosen to be 15%. The specimens were saturated and then isotropically consolidated to the mean effective pressures between 100-400 kPa. After consolidation, specimens were subjected to undrained monotonic strain-controlled triaxial compression loadings with a constant strain rate of 0.01mm/min.

The following figures (Figure 5, 6 and 7) show the results of performed triaxial tests. The effective stress paths in *p'-q* plane, the deviator stress-axial strain curves and pore pressure ratio-axial strain curves of contractive samples are shown in Figures 5a, 6a and 7a, respectively. Pore pressure ratio, r_u is defined as the ratio between excess pore pressure and mean effective pressure after consolidation. In Figure 5a, the steady state line (SSL) of contractive samples is also depicted. It has a slope (M) in *p'-q* plane equal to 1.36. The same line (SSL) is added also in Figure 5b for comparison with dilative samples. Figures 5b, 6b and 7b show the effective stress paths in *p'-q* plane, the deviator stress-axial strain curves and pore pressure ratio-axial strain curves of dilative samples, respectively. Void ratios after consolidation (e) are also included on Figures 5a and 5b. We believe that significant changes of stress path slopes at the end of plots in Figure 5b were due to strain localization in shear bands. Therefore, the steady states could not be reached completely. Steady state line (SSL) in *e-p'* plane is presented in Figure 8 along with isotropic compression lines (ICL). It can be observed that the slope of SSL is much steeper than the slopes of the ICLs. The reason for this difference probably lies in insufficiently high stresses in isotropic compression to reach a unique normal compression line (in the same way as in Figure 4). Similar difference in slopes can be found in literature (e.g. Thevanayagam and Mohan, 2000; Yang, 2004), while the cause of the difference could be the effect of fines. Additionally in Figure 8, SSLs of silty sands with 30% fines content (FC) from some other researchers are depicted for inclination comparison. It can be seen that SSLs can have similar (Bouckovalas et al., 2003; Naeini and Baziar, 2004) or less steep (Yang, 2004; Zlatovic and Ishihara, 1995) inclination than the one we present.

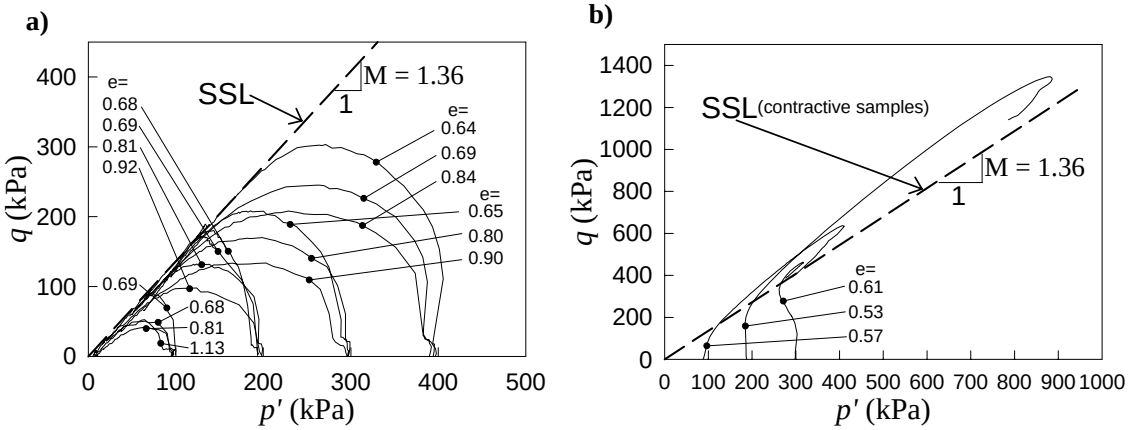

Figure 5. Effective stress paths of contractive (a) and dilative (b) samples along with the steady state line (SSL) of contractive samples and void ratios (*e*) after consolidation.

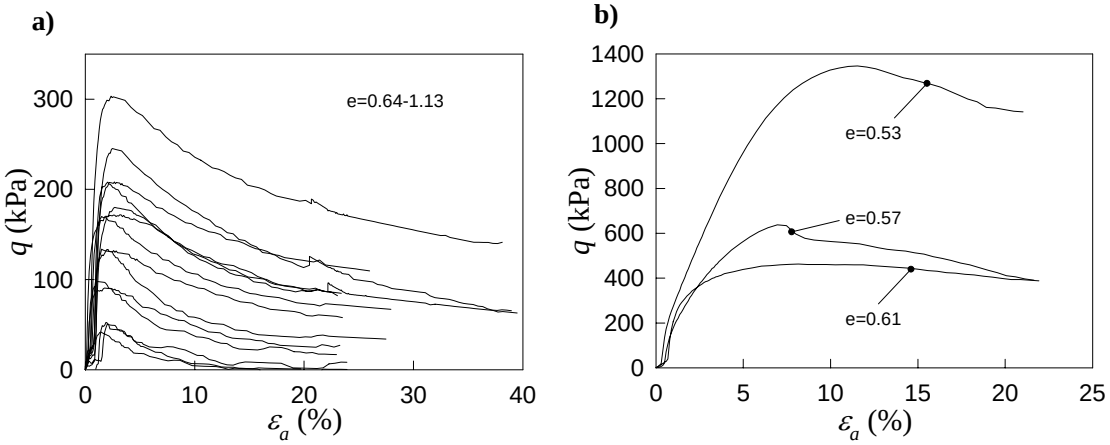

Figure 6. Deviator stress-axial strain curves of contractive (a) and dilative (b) samples

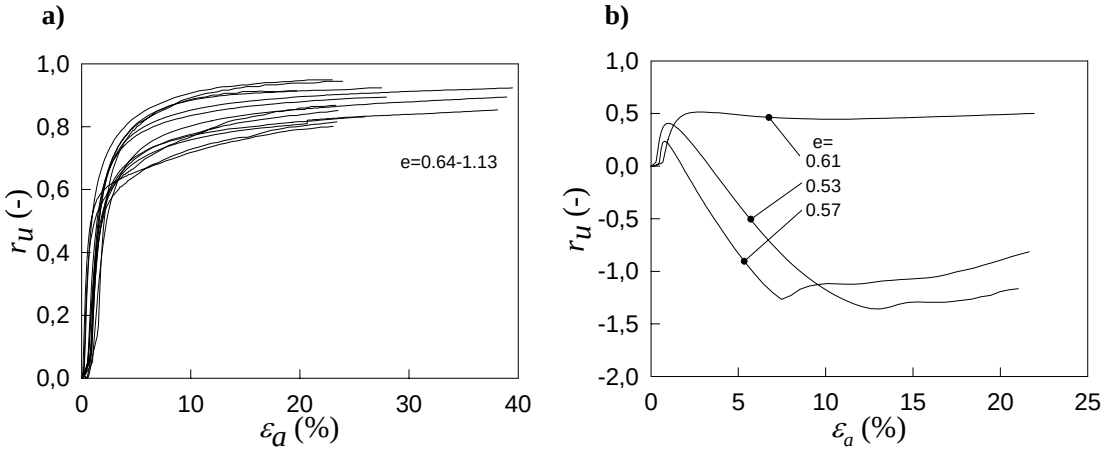

Figure 7. Pore pressure ratio-axial strain curves of contractive (a) and dilative (b) samples

Another characteristic that can be observed from the steady states in *e-p'* plane is their possible dependence on the stress level (Thevanayagam and Mohan, 2000). Therefore, in Figure 9 the steady states are divided into three distinctive SSLs, according to the effective confining pressure after consolidation. On the other hand, the steady states could have been divided into three SSLs according to different void ratio levels (the density effect). The SSLs from Thevanayagam and Mohan (2000) are

also drawn in Figure 9 for comparison. Similar trend with increasing effective confining pressure can be observed.

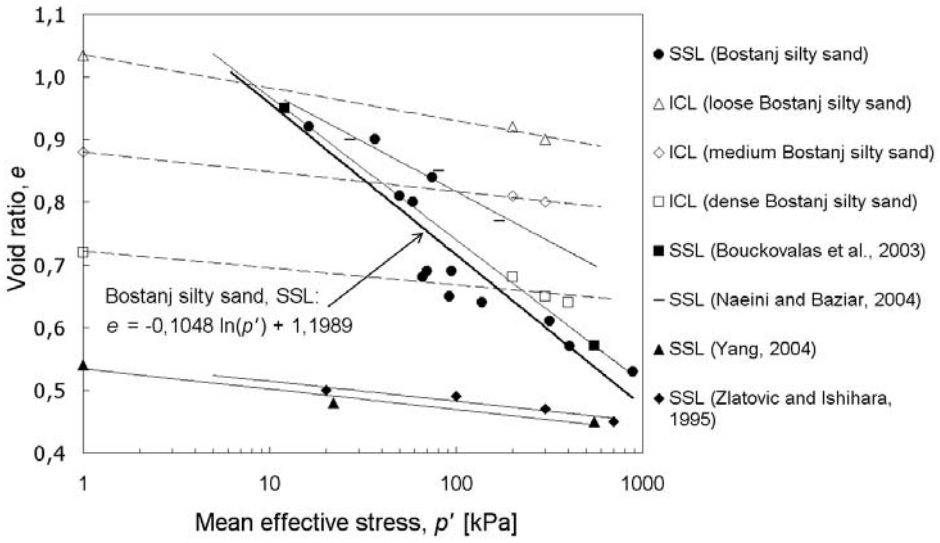

Figure 8. Steady state line (SSL-bold solid plot) and istropic consolidation lines (ICL-dashed plot) of Bostanj silty sand compared to SSLs (solid plot) of some other silty sands with FC=30%. Equation of Bostanj silty sand SSL is also presented.

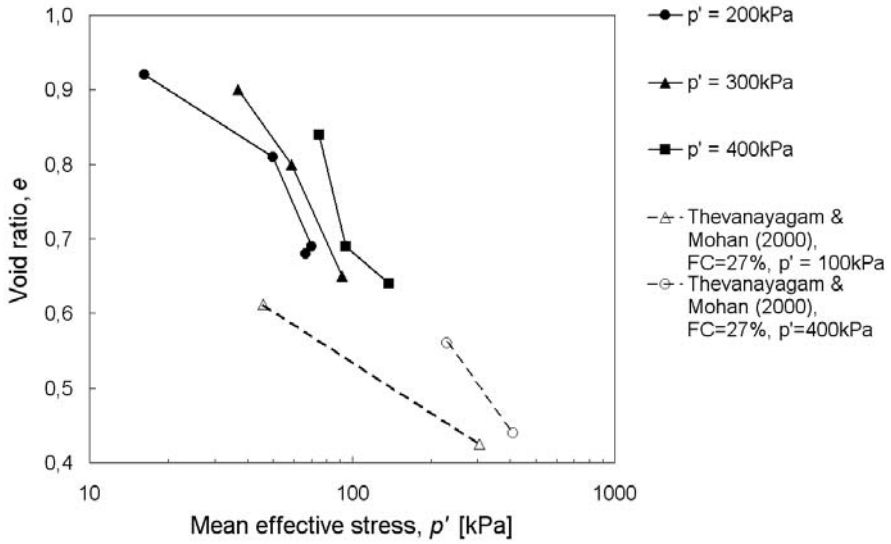

Figure 9. Steady states of Bostanj silty sand divided into three distinctive SSLs (solid plots) according to the effective confining pressure (*p'*) after consolidation and two SSLs (dashed plots) from Thevanayagam & Mohan (2000) according to different *p'*.

Bender element tests

In order to determine small-strain stiffness of Bostanj silty sand and its dependence on effective confining pressure, bender element tests were perfomed in the triaxial cell. The specimen dimensions were 70 mm in diameter and 140 mm in height. Water content was 20%. The procedure used to perform the bender element tests was the multistage technique, with different effective confining stress magnitudes being applied. After each consolidation step the longitudinal (v_p) and shear wave velocities

(v_s) were measured using bender elements and corresponding small strain shear stiffness (G_0) was calculated. Then an empirical relation

$$G_0 = A \cdot \frac{(2.17 - e)^2}{1 + e} (\sigma'_0)^n \quad (1)$$

proposed by Hardin (1978) was utilized to plot the dependence of G_0 on effective confining stress σ_0', taking into account the consolidation void ratio e. A and n are constants that depend solely on the particular soil. The relation between G_0 and σ_0' using Equation 1 is shown in Figure 10 for Bostanj silty sand. Additionally, the results for clean Ottawa sand and Ottawa sand with 20% silt (Salgado et al., 2000) using Equation 1 are also depicted in the same figure for comparison. The parameters chosen to get the best fit for Bostanj silty sand were A=2000 and n=0.65. Salgado et al. (2000) proposed the values of A=8105; n=0.439 and A=498.9; n=0.809 for clean Ottawa sand and Ottawa sand with 20% silt, respectively. It can be seen in Figure 10, that increasing fines content reduces the slope of G_0-σ_0' curves.

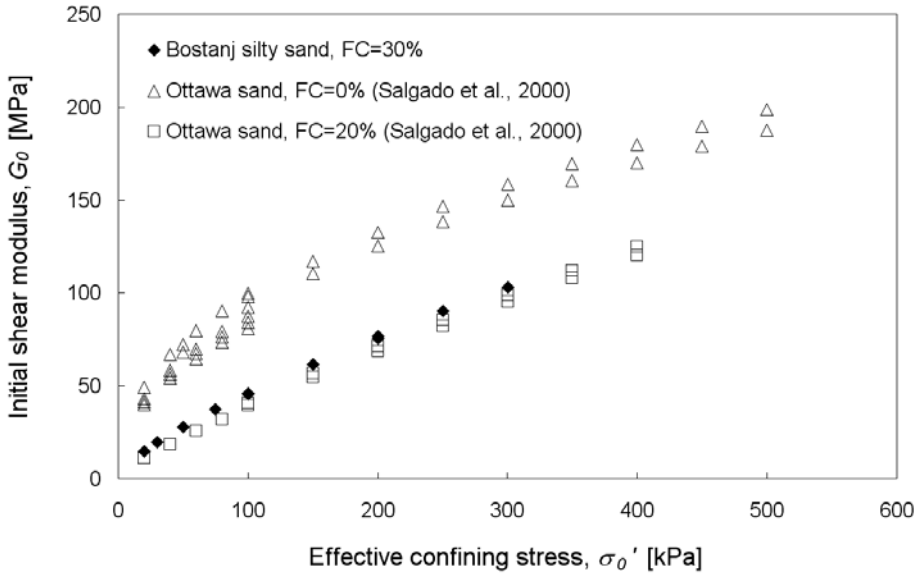

Figure 10. Results of bender element tests of Bostanj silty sand compared to the results of clean Ottawa sand and Ottawa sand with 20% of fines (Salgado et al., 2000)

Cyclic tests

In order to study the sensitivity of the material to cyclic mobility a series of undrained cyclic triaxial and cyclic simple shear tests was carried out. All of the tests were conducted on reconstituted saturated specimens of Bostanj silty sand (FC = 30%). Specimens were moistly tamped in layers. The triaxial specimens were 70 mm in diameter and 140 mm in heigth and simple shear specimens were 70 mm in diameter and 30 mm in height. The frequency of loading was 1-2 Hz for triaxial specimens and 0.5 Hz for simple shear specimens. All the specimens were isotropically consolidated to effective confining pressure of 75 kPa and then cyclically sheared with stress reversals. Because of the isotropic consolidation (K_0=1) no correction factor were used (Das, 1992) to compare the results of cyclic triaxial and cyclic simple shear tests. Consolidated void ratios e varied within 0.61-0.72, while the range of cyclic stress ratios (CSR) was 0.20-0.38 and 0.10-0.15 for triaxial and simple shear tests, respectively. The number of cycles to liquefaction (N_c) was identified when double strain amplitude reached 5% or when the pore pressure become equal to the initial effective confining pressure ('initial liquefaction'). Figure 11 shows the results of CSR versus N_c for both kinds of cyclic tests. The results with e=0.61-0.64 and e=0.72 form a pronounced curve, while there is a lack of a clear trend in the range of e=0.66-0.68. The area between both curves presents the expected liquefaction resistance of

the field material, while the in-situ void ratios vary between 0.63 and 0.72 (Table 1). For comparison, *CSR*-N_c data for different sands with 30% silt content are shown from Xenaki & Athanasopoulos (2003) and Tronsco & Verdugo (1985). They used cyclic triaxial testing device. Shinias-Marathon sand with void ratio e=0.62-0.69 (Xenaki and Athanasopoulos, 2003) and Tailing sand with void ratio e=0.85 (Tronsco & Verdugo, 1985) were tested, both at confining pressure p'=200 kPa. Similar trends can be observed comparing to our results.

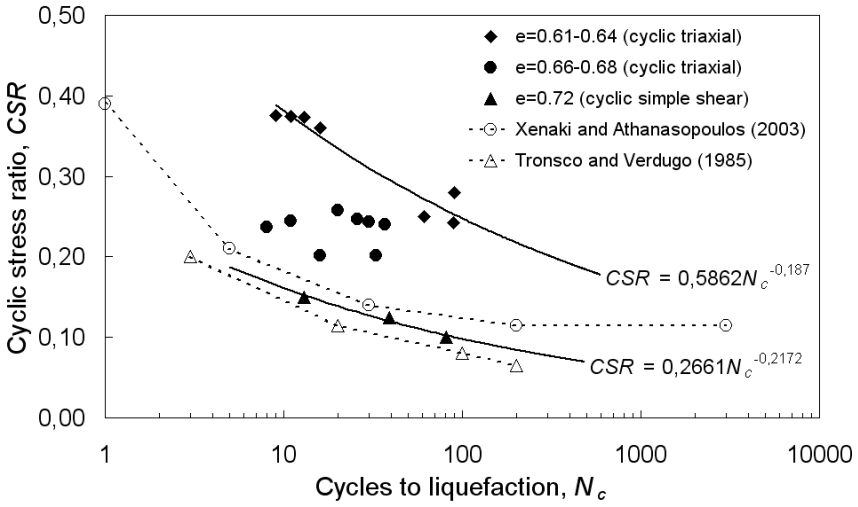

Figure 11. *CSR* versus N_c for Bostanj silty sand in cyclic simple shear and cyclic triaxial conditions at different void ratio values. For comparison, *CSR* versus N_c curves are shown from Xenaki & Athanasopoulos (2003) and Tronsco & Verdugo (1985).

MODELLING OF INSTABILITY POINTS

The measured amplitude of three-dimensional accelerations in the layer of silty sand caused by train passings did not exceed the value of 0.095g. Therefore, it was concluded that train loading can not cause the cyclic mobility or trigger the liquefaction failure. On the other hand, earthquakes of medium magnitude (up to M=6.5) are expected in Bostanj area. Therefore, further laboratory tests were carried out to define the conditions that can cause liquefaction of silty sand layer. Direct shear tests were conducted in order to get the regions of dilative and contractive behaviour. If the in-situ void ratio is taken to be between 0.63-0.72 (Table 1) and maximum effective vertical stress σ_v' is 75-100 kPa, then the in-situ state of material is above and below the critical state line from direct shear tests in e-logσ_v' plane (Figure 4). Therefore, during shearing, both contractive and dilative responses are expected.
Moreover, if we take the maximum mean effective stress p' to be around 100 kPa according to static analysis with FLAC and again take in-situ void ratio to be between 0.63-0.72, the in-situ state of the material is again on or near the steady/critical state line from undrained triaxial tests in e-logp' plane (Figure 8). Therefore, contractive or dilative response can be expected during shearing. Another important feature are stress states of in-situ material transformed to invariant p'-q plane. If maximum p' and q taken from static analysis with FLAC are both around 100 kPa, the stress state of the material is plotted close to the peak/instability line from undrained triaxial compression tests with similar range of void ratios between 0.63-0.72 (Figure 12). Irrespectively of considerable scatter of instability line data, the possibility of flow liquefaction failure can not be excluded.

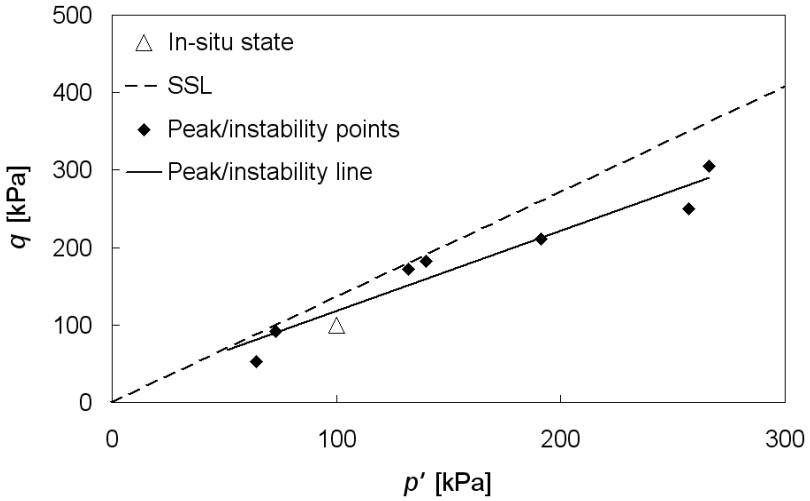

Figure 12. SSL (M=1.36) and peak/instability line from undrained triaxial compression tests on contractive samples along with the proposed most unfavourable in-situ stress state, which was transformed to stress invariants *p'* and *q*

According to the test results of undrained triaxial compression tests on contractive samples, a simple relation is derived, connecting the peak deviator stress (q_{peak}) and peak mean effective stress (p'_{peak}) with mean effective stress after consolidation (σ_c') and the state parameter (ψ_0).

$$q_{peak} = \sigma_c'^{(a-\psi_0)} + \sigma_c' \cdot b \tag{2}$$

$$p'_{peak} = \sigma_c'^{(c-\psi_0)} + \sigma_c' \cdot d \tag{3}$$

The state parameter ψ_0 is the void ratio difference between the initial state (before triaxial compression) and the steady state conditions (SSL) at the same mean effective stress. The state parameter was introduced by Wroth & Bassett (1965). The material parameters a, b, c and d for Bostanj silty sand are given in Table 3 and were chosen to give the best fit to the experimental data. The predictions calculated by using equations (2) and (3) along with the actual peak points are depicted in Figure 13.

Table 3. Parameters of the equations (2) and (3) for Boštanj silty sand.

Parameter	Value
a	0.90
b	0.41
c	0.70
d	0.57

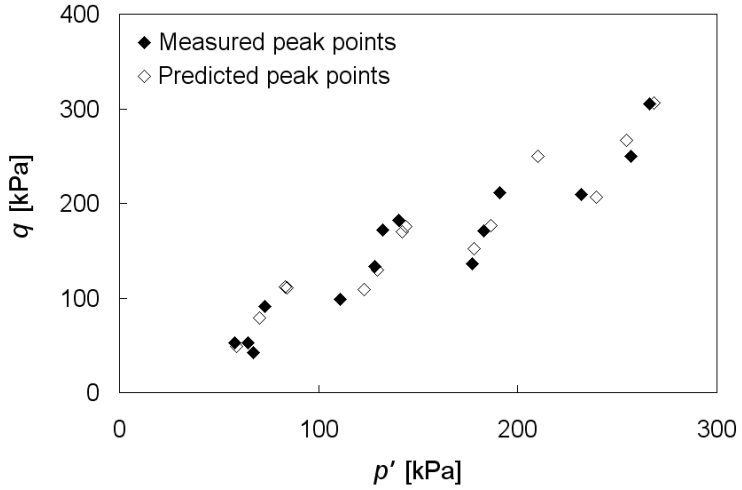

Figure 13. Comparison of the actual and predicted peak points according to proposed equations (2) and (3)

CONCLUSIONS

The results of the field and laboratory tests of the silty sand from the railway embankment were presented in the paper. The main aim of the tests was to examine the liquefaction susceptibility of the material which was planned to be submerged due to the construction of the accumulation reservoir.
Based on the experimental results of the current study, the following conclusions can be drawn:

1. The measured accelerations caused by the railway traffic are too low to cause the liquefaction in the silty sand layer.
2. The in-situ state of the silty sand material, according to the in-situ void ratio and the most unfavourable stress state, is very close to the critical state line in *p'*-*e* plane derived from undrained monotonic triaxial test and also close to the critical state line in *e*-logσ_v' plane derived from direct shear tests. Moreover, the most unfavourable stress state transformed to invariants *p'* and *q* is close to the peak/instability line in *p'*-*q* plane from undrained triaxial tests. Therefore, it is concluded that contractive behaviour of the in-situ silty sand is possible during earthquake loading, while flow liquefaction trigerring also can not be excluded.
3. The simple relation was proposed from the results of undrained triaxial tests on contractive samples. It connects the peak deviator stress and peak mean effective stress with mean effective stress after consolidation and state parameter of the initial state. The relation has to be validated with the extension of the monotonic undrained tests.
4. Cyclic triaxial and cyclic simple shear tests showed that the studied material is susceptible to cyclic mobility.
5. In further work the additional series of cyclic and monotonic triaxial tests will be carried out. The aim of the tests is to reduce the uncertainty in *CSR*-N_c plots and more accurately define the steady state line. Results of high pressure triaxial tests are supposed to be used for more certain steady state definition.

ACKNOWLEDGEMENTS

Authors wish to thank Holding Slovenske elektrarne (HSE) for the financial support of a part of the investigations. The valuable help of collaborators from Slovenian National Building and Civil Engineering Institute (ZAG), Prof. J. Logar of the Faculty of civil and geodetic engineering in Ljubljana and Prof. B. Žlender of the Faculty of civil engineering in Maribor during the experimental

part of the work is appreciated. The financial support of the Ministry of Higher Education, Science and Technology, Slovenia is gratefully acknowledged.

REFERENCES

Bouckovalas GD, Andrianopoulos KI, Papadimitriou G (2003). A critical state interpretation for the cyclic liquefaction resistance of silty sands. *Soil dynamics and Earthquake Engineering*, 23, pp. 115-125

Castro G (1975). Liquefaction and cyclic mobility of saturated sands. *Journal of the Geotechnical Engineering Division*, ASCE, 101, pp. 551-569

Castro G, Poulos SJ (1977). Factors affecting liquefaction and cyclic mobility. *Journal of the Geotechnical Engineering Division*, ASCE, 103, pp. 501-516

Das, BM. (1992). *Principles of soil dynamics*. PWS-KENT Publishing Company, Boston, Massachusetts, 397-459

Ishihara K (1993). Liquefaction and flow failure during earthquakes. *Geotechnique*, 43, pp. 351-415

Hardin BO (1978). The nature of stress-strain behavior of soils. *Proc. Earthquake Engineering and Soil Dynamics Conference*, Pasadena, ASCE, pp. 3-90

Lade PV, Yamamuro JA (Editors) (1999). *Physics and mechanics of soil liquefaction*. A.A. Balkema, Rotterdam

Lapajne J, Sket Motnikar B, Zupancic P (2001). The new map of seismic danger – design ground accelerations intead of intensity. *Gradbeni vestnik*, 50, pp. 140-149 (in Slovene)

Lenart S, Petkovsek B (2006). Assessment of liquefaction potential of a loose soil in the base of a railroad, *Proceedings of the XIIIth Danube European Conference on Geotechnical Engineering*, Ljubljana, Vol. 2, 965-970

Lenart S, Fifer Bizjak K, Petkovsek B (2005). Report on the dynamic analysis of the critical cross section of the railway line at Bostanj accumulation basin. ZAG, P 810/05-750-2 (in Slovene)

Naeini SA, Baziar MH (2004). Effect of fines content on steady-state strength of mixed and layered smaples of sand. *Soil dynamics and earthquake engineering*, Vol.24, No.3, pp. 181-187

Salgado R, Bandini P, Karim A (2000). Shear strength and stiffness of silty sand. *J. Geotech. Geoenviron. Eng.*, Vol. 126, No. 5, pp. 451-462

Seed, HB, Lee, KL 1966. Liquefaction of saturated sands during cyclic loading. *Journal of the Soil Mechanics and Foundations Division*, ASCE, Vol. 92, No. SM6, pp. 105-134

Schofield AN, Wroth CP (1968). *Critical state soil mechanics*. McGraw-Hill, London

Thevanayagam S, Mohan S (2000). Intergranular state variables and stress-strain behaviour of silty sands. *Geotechnique*, 50(1), pp. 1-23

Tronsco JH, Verdugo R (1985). Silt content and dynamic behavior of tailing sand. *Proc. Twelfth International Conference on Soil Mech. And Found. Eng.*, San Francisco, USA, pp. 1311-1314

Wroth CP, Bassett RH (1965). A stress-strain relationship for the shearing behaviour of a sand, *Geotechnique*, 15, No. 1, pp. 32-56

Xenaki VC, Athanasopoulos GA (2003). Liquefaction resistance of sand-silt mixtures: an experimental investigation of the effect of fines. *Soil dynamics and earthquake engineering*, 23, pp. 183-194

Yamamuro JA, Lade PV (1998). Steady-state concepts and static liquefaction of silty sands. *Jorunal of Geotechnical and Geoenvironmental Engineering*, Vol. 124, No. 9, pp. 868-877

Yang S (2004). Characterization of the properties of sand-silt mixtures. Ph.D Thesis, Norwegian University of Science and Technology

Zlatovic S, Ishihara K (1995). On the influence of nonplastic fines on residual strength. *Proceedings 1st Int. Conf. on Earthq. Geotech. Engrgr.*, Ishihara (ed), Balkema, Rotterdam, pp. 239-244